

RESEARCH ARTICLE

10.1002/2016JC012521

Key Points:

- Wave model simulations based on CMIP5 forcing covering the northeast Atlantic
- Projected decrease in significant wave height by the end of the 21st century
- Largest decline is obtained with the RCP8.5 scenario

Correspondence to:

O. J. Aarnes,
ole.aarnes@met.no

Citation:

Aarnes, O. J., M. Reistad, Ø. Breivik, E. Bitner-Gregersen, L. Ingolf Eide, O. Gramstad, A. K. Magnusson, B. Natvig, and E. Vanem (2017), Projected changes in significant wave height toward the end of the 21st century: Northeast Atlantic, *J. Geophys. Res. Oceans*, 122, 3394–3403, doi:10.1002/2016JC012521.




Received 1 NOV 2016

Accepted 22 MAR 2017

Accepted article online 28 MAR 2017

Published online 26 APR 2017

Projected changes in significant wave height toward the end of the 21st century: Northeast Atlantic

Ole Johan Aarnes¹ , Magnar Reistad¹ , Øyvind Breivik^{1,2} , Elzbieta Bitner-Gregersen³, Lars Ingolf Eide⁴ , Odin Gramstad³ , Anne Karin Magnusson¹, Bent Natvig⁵ , and Erik Vanem^{3,5} 

¹Norwegian Meteorological Institute, Bergen, Norway, ²Geophysical Institute, University of Bergen, Bergen, Norway, ³DNV GL Strategic Research and Innovation, Høvik, Norway, ⁴Eide Environmental Consultant, Rykkinn, Norway, ⁵Department of Mathematics, University of Oslo, Oslo, Norway

Abstract Wind field ensembles from six CMIP5 models force wave model time slices of the northeast Atlantic over the last three decades of the 20th and the 21st centuries. The future wave climate is investigated by considering the RCP4.5 and RCP8.5 emission scenarios. The CMIP5 model selection is based on their ability to reconstruct the present (1971–2000) extratropical cyclone activity, but increased spatial resolution has also been emphasized. In total, the study comprises 35 wave model integrations, each about 30 years long, in total more than 1000 years. Here annual statistics of significant wave height are analyzed, including mean parameters and upper percentiles. There is general agreement among all models considered that the mean significant wave height is expected to decrease by the end of the 21st century. This signal is statistically significant also for higher percentiles, but less evident for annual maxima. The RCP8.5 scenario yields the strongest reduction in wave height. The exception to this is the north western part of the Norwegian Sea and the Barents Sea, where receding ice cover gives longer fetch and higher waves. The upper percentiles are reduced less than the mean wave height, suggesting that the future wave climate has higher variance than the historical period.

1. Introduction

Wind-generated surface waves are increasingly seen as an essential variable in climate prediction [Hemer *et al.*, 2012], both as an important modulator of the air-sea exchange [Cavaleri *et al.*, 2012; Fan and Griffies, 2014; Breivik *et al.*, 2015] and for its importance to marine and coastal safety, e.g., by coastal erosion, flooding, offshore, and shipping design. However, with a few exceptions [Fan and Griffies, 2014; Li *et al.*, 2016], coupled climate models do not yet incorporate wave models. So in order to obtain future wave climate statistics, a standalone wave model integration forced by projected surface winds is needed [Hemer *et al.*, 2013; Hemer and Trenham, 2016], or some statistical approach utilizing already existing output parameters as a predictor for waves [Wang *et al.*, 2014]. Either way, the wave data will rely heavily on the performance of the parent climate model.

The Coupled Model Intercomparisons Project Phase 5 (CMIP5) comprises climate models that form the scientific basis for the Fifth Assessment Report on Climate Change (AR5) of the Intergovernmental Panel on Climate Change (IPCC) [Stocker *et al.*, 2014]. By defining a standardized set of experiments, CMIP5 provides a framework for comparing and evaluating climate models. In total, four different scenarios are adopted in AR5, also known as Representative Concentration Pathways (RCPs). The RCPs represent possible future greenhouse gas concentration trajectories, where the associated number, i.e., RCP2.6, RCP4.5, RCP6.0, and RCP8.5, reflects the expected radiative forcing near the tropopause [W/m^2] comparing the year 2100 against the preindustrial era. In general, each RCP is linked with a likely climate scenario, where some of the more confident predictions are presented in the IPCC AR5 Synthesis Report [Pachauri *et al.*, 2014]. Typically, these are related to global warming, regional increases/decreases in precipitation, retreating sea ice cover in the Arctic, and sea level rise. Despite a fair level of agreement among the majority of CMIP5 models regarding such key aspects, projections of other climate variables are more uncertain. In terms of future wave climate, the IPCC AR5 is inconclusive due to a reported “knowledge gap” in the current understanding [Barros *et al.*, 2014]. This is well illustrated by Wang *et al.* [2015], who performed an analysis of variance on

significant wave height data obtained with a statistical model utilizing CMIP5-winds from a 20-model ensemble. They found that the intermodel variability was significant globally and about 10 times larger than the difference between scenarios RCP4.5 and 8.5. Other notable global studies include *Dobrynin et al.* [2012], *Semedo et al.* [2012], *Fan et al.* [2013], *Mori et al.* [2013], *Hemer et al.* [2013], *Wang et al.* [2014], *Fan et al.* [2014], *Hemer and Trenham* [2016], and *Shimura et al.* [2015a]. Regional studies on higher resolution have also recently appeared for the Arctic Ocean [*Khon et al.*, 2014], the Atlantic Ocean [*Grabemann et al.*, 2015; *Perez et al.*, 2015; *Martinez-Asensio et al.*, 2016; *Gallagher et al.*, 2016], the Pacific [*Erikson et al.*, 2015; *Shimura et al.*, 2015b,2016], and the Mediterranean [*Casas-Prat and Sierra*, 2013].

In order to quantify model uncertainties associated with future wave climate projections, we here consider a range of CMIP5 models. Ideally, the ensemble should be a selection of models that faithfully reconstruct past wave climate, i.e., capturing any changes brought about by emissions respective to the preindustrial era, but still expected to vary within the range of natural variability. However, since such an evaluation can only be done *after* forcing a wave model with surface winds from the climate model in question, we have instead chosen to assess the climate model performance on their ability to recreate past wind and storm track climate.

The wave climate of the midlatitudes is closely related to the extratropical cyclone activity. A teleconnection pattern like the North Atlantic Oscillation (NAO) [*Hurrell*, 1995], represented by the NAO-index, exhibits a correlation coefficient of 0.9 against mean wintertime significant wave height west of the British Isles [*Shimura et al.*, 2013]. Unlike the swell-dominated Tropics, waves in the northeast Atlantic are strongly correlated with the local wind speed, and even more so than in the midlatitudes of the Southern Hemisphere [*Stopa et al.*, 2013]. This implies that any projected changes in the future wave climate are closely linked to the individual climate model's ability to represent realistic extratropical cyclone activity, in terms of tracks, intensity, and number.

Climate models remain relatively coarse compared to numerical weather prediction (NWP) models and are limited in their ability to model the intensity and evolution of extratropical storms. However, *Zappa et al.* [2013a] show that CMIP5 models have improved performance over CMIP3 in terms of storm tracks, in particular in the North Atlantic where the northeastward tilt of the storm tracks is better captured, i.e., the extension of low pressure tracks from South of Greenland into the Norwegian Sea. Even so, the majority of CMIP5 models continue to push too many cyclones toward Europe rather than into the Norwegian Sea. The average cyclone intensity is also too weak, which is a particular concern when the emphasis is on extremes [*Breivik et al.*, 2014]. Nevertheless, some of the better resolved models show better agreement with observed storm tracks and low pressure intensity [*Zappa et al.*, 2013a], adding confidence to the current study, where models of higher spatial resolution have been given preference. In a related study by *Perez et al.* [2014], the performance of CMIP3 versus CMIP5 models is evaluated using a synoptic classification routine. Based on sea level pressure (1950–1999) from the NCEP/NCAR Reanalysis I [*Kalnay et al.*, 1996], the 100 most prominent weather types are distinguished using a combination of principal component analysis and *k*-means clustering analysis. By conducting the same analysis based on climate models over the same historical period, the relative frequencies of weather types are evaluated. In general, the analysis reveals that the best CMIP5 models perform better than the earlier CMIP3 models, but that performance varies with season. *Perez et al.* [2014] further stress the importance of using ensembles or multimodel ensembles to better represent the uncertainty associated with future climate projections.

In this study, we use near-surface (10 m) winds obtained from six CMIP5 models to force the wave model WAM [*Komen et al.*, 1994] over the historical period 1971–2000 and a future period (2071–2100) on a domain covering the northeast Atlantic. The paper is organized as follows. First, the model setup and the forcing data are presented in section 2. In section 3, the different wave model simulations are compared against a high-resolution wave hindcast, NORA10 [*Reistad et al.*, 2011], and thereafter used to investigate future projected changes in significant wave height. Section 5 offers concluding remarks.

2. Model Integrations

We use the wave model WAM [*Group*, 1988; *Komen et al.*, 1994], Cycle 4. The model is run with a directional resolution of 15° and 25 frequencies, spanning the frequency domain 0.0420–0.4137 Hz with logarithmic 10% increments. The model is set up on a rotated spherical grid with approximately 50 km resolution,

Table 1. The CMIP5-Models Used in the Study, Providing Near-Surface Winds (3 Hourly) and Sea Ice Concentration (Updated Monthly) for the WAM50 Simulations^a

Model	Resolution		Period		Member
	(Lon/Lat)				
EC-Earth	1.125° × 1.125°		1971–2000	2071–2100	2/9/12
HadGEM2-ES	1.875° × 1.25°		1970–1999	2081–2099	1
IPSL-CM5A-MR	2.5° × 1.25°		1971–1999	2071–2099	1
GFDL-CM3	2.5° × 2.0°		1970–1999	2071–2100	1
MIROC5	1.4° × 1.4°		1971–1999	2070–2099	1/2/3
MRI-CGCM3	1.125° × 1.125°		1971–2000	2071–2100	1

^aEach model is represented by their horizontal resolution, the extracted historical/future period, and the corresponding member numbering available at the ESGF database at the time of the study.

covering the northeast Atlantic, see Figure 3. This is identical to the coarser (outer) domain described by *Reistad et al.* [2011]. Boundaries are closed, with no swell entering the model domain, with parametric, wind-dependent spectra [*Hasseilmann et al.*, 1973] applied on the boundaries. This deteriorates the model performance near the boundaries but has limited impact elsewhere as the model domain covers the majority of North Atlan-

tic Open Ocean influenced by extratropical cyclones. The wave model is run with a 15 min time step. Winds are updated every 3 hours and linearly interpolated in time. Ice cover is updated monthly and kept constant over the month.

The wave model integrations are forced by near-surface (10 m) winds and confined by the sea ice concentration, both parameters that are available from climate models in CMIP5. Besides a historical period, two future greenhouse gas concentration scenarios, or Representative Concentration Pathways (RCPs) [*Taylor et al.*, 2012], have been studied, namely RCP4.5 and RCP8.5. The six selected models are listed in Table 1. All data have been retrieved from the Earth System Grid Federation (ESGF) database, with the exception of EC-Earth, which was made accessible by the Swedish Meteorological and Hydrological Institute (K. Wyser, personal communication, 2015). Only models providing 3-hourly winds were considered and models with relatively high spatial resolution were preferred. The number of extracted ensemble members per model varies somewhat depending on availability at ESGF. The forcing fields were interpolated bilinearly to the WAM 50 km model domain, hereafter referred to as WAM50. Altogether, the historical and future wave model integrations amount to about 1000 simulated years.

3. Model Evaluation

To evaluate the WAM50/CMIP5 integrations, the historical runs were compared against NORA10, a high-resolution atmospheric downscaling of ERA-40 and wave hindcast [*Reistad et al.*, 2011; *Uppala et al.*, 2005]. See also *Aarnes et al.* [2012], *Furevik and Haakenstad* [2012], and *Breivik et al.* [2013]. Figure 1 displays the deviation in mean H_s between NORA10 (1971–2000) and the six WAM50/CMIP5 ensembles covering the historical periods listed in Table 1. Blue colors indicate a negative bias relative to NORA10, while red represents a positive bias. Maximum ice extent from each model ensemble and NORA10 is marked by black and dark red lines, respectively. Overall, the most conflicting results are obtained with IPSL-CM5A-MR, which is excessively low [*Dufresne et al.*, 2013], and MRI-CGCM3, which is too high relative to NORA10 in ice-free areas. In addition, both models portray an unrealistic maximum ice extent. HadGEM2-ES and GFDL-CM3 perform better but are still low, especially in coastal areas. EC-Earth and MIROC5 show the best agreement with the NORA10 hindcast. Although both models show slightly elevated wave heights in the western part of the model domain, this is mainly an artifact of the poorer performance of NORA10 near the western boundaries, an area where the hindcast is biased low due to the influence of the ERA-40 boundary [*Aarnes et al.*, 2012]. MIROC5 appears somewhat more influenced by land, illustrated by the reduced mean wave conditions near the coast and in the Baltic Sea. Otherwise, both models are mainly within ± 0.2 m of NORA10.

A similar comparison of the mean annual maximum H_s is presented in Figure 2. The result is more or less in line with the findings made above. EC-Earth captures the extremes slightly better than the other models, but HadGEM2-ES is also quite good. MIROC5 is now showing the best compliance near the coast, in controversy to Figure 1, and too high levels in the open ocean. This general elevated state of the extremes, compared to the means, may indicate an excessive spread in the wind climate simulated by MIROC5. IPSL-CM5A-MR and MRI-CGCM3 exhibit substantial biases relative to NORA10. Common to all models is an expanded maximum ice extent.

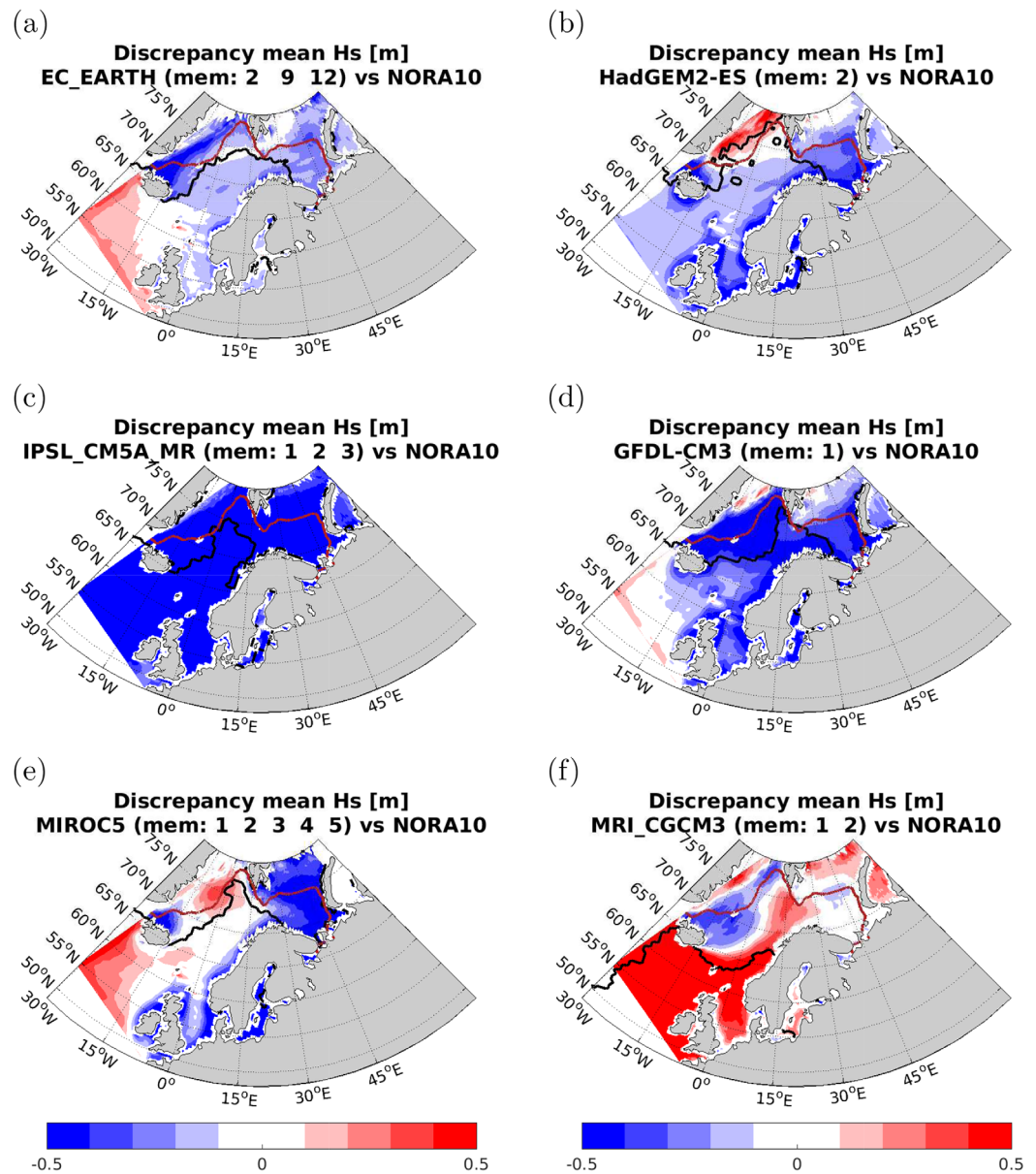


Figure 1. Discrepancy in mean significant wave height (m) between the WAM50/CMIP5 integrations (1971–2000) and NORA10 (1971–2000). The maximum ice extent is marked by the black and dark red lines, representing the different WAM50/CMIP5 ensembles and NORA10, respectively. (a–f) Correspond to the models listed in Table 1.

4. Future Projections

We now combine all WAM50/CMIP5 simulations in one model ensemble, where each model is given equal weight by first averaging the ensemble members for each model. Since each CMIP5 model produces different mean wave conditions (see Figure 3), the data are first normalized against that model’s historical climate before merging the data sets. The analysis has been conducted as follows. First, annual statistics from each model member have been extracted, i.e., mean, 90 percentile (p90), 99 percentile (p99), and annual maxima. Second, an annual ensemble mean per model is constructed from the annual statistics. In this way, each model is represented by the number of nonoverlapping years and thus independent of the number of ensemble members. All runs, with the exception of HadGEM2-ES, cover ~30 years over the historical and future period, respectively. Since HadGEM2-ES only covers the period 2081–2099, the model is weighted slightly less in the model ensemble. Third, all annual data are normalized by the corresponding mean

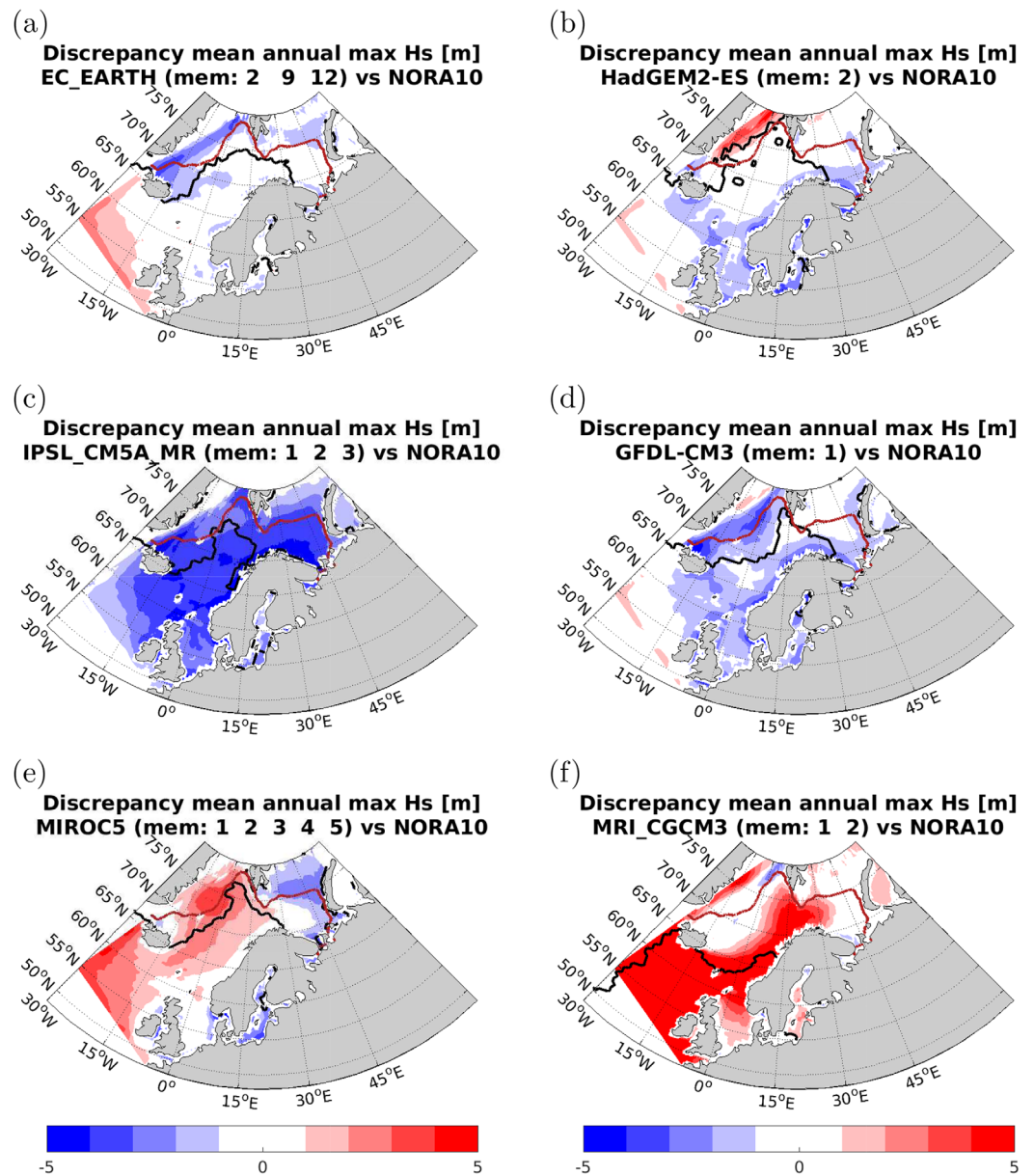


Figure 2. Discrepancy in mean annual maximum significant wave height (m) between the WAM50/CMIP5 historical integrations (1971–2000) and NORA10 (1971–2000). The maximum ice extent is marked by black and dark red lines, representing the different WAM50/CMIP5 ensembles and NORA10, respectively. (a–f) Correspond to the models listed in Table 1.

statistics from the historical period and the respective model. In other words, all annual data, historical and future, are represented by the anomalies relative to each model’s historical climate, i.e.,

$$\frac{H_t - \bar{H}_{\text{Hist}}}{\bar{H}_{\text{Hist}}} \times 100, \tag{1}$$

where H_t represents an annual statistic (mean, p90, p99, and annual max) of significant wave height based on each model, averaged across all members available per year (t) over the historical or future period, respectively. \bar{H}_{Hist} represents the mean of the annual statistic over the historical period per model.

When averaging the annual anomalies associated with each scenario, the expected future change is obtained. In order to establish whether the estimated changes are statistically significant, we have conducted a two-sample t test between the historical and future annual anomalies, at a significance level of

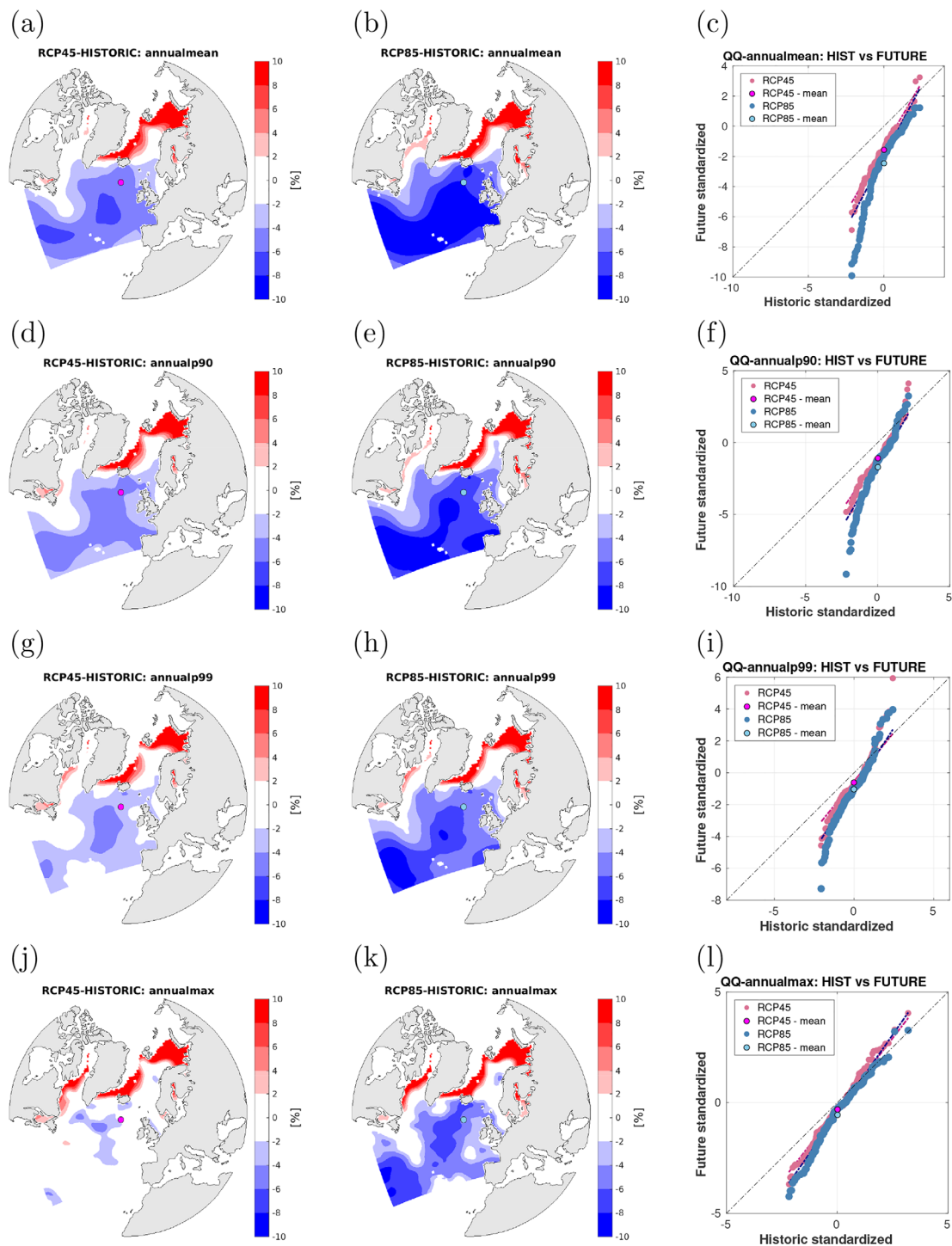


Figure 3. Change in significant wave height between the periods 2071–2100 and 1971–2000 given as a percentage relative to the historical period. Wave model integrations are forced with winds from six CMIP5 models under two climate scenarios, (a, d, g, and j) RCP4.5 and (b, e, h, and k) RCP8.5, see also Table 1. Here each WAM50/CMIP5 is represented by the ensemble mean, i.e., each model is weighted equally (except HadGEM2-ES which is based on a truncated future period). Colored areas have significant differences ($\alpha = 5\%$). Figures 3a and 3b reveal that RCP8.5 sees a greater decrease in long-term mean significant wave height, except in the areas that were previously ice-covered during winter. This is also the case for upper percentiles (compare Figures 3d and 3e for the 90th percentile and Figures 3g and 3h for the 99th percentile). The annual maxima maps (Figures 3j and 3k) show that RCP4.5 has virtually no reduction compared to the historical period while RCP8.5 shows significant reduction. Standardized quantile-quantile plots of historical versus future climate for the two scenarios in a location in the North Atlantic (marked with a red or blue dot in the maps) are shown for (c) annual mean values, (f) annual 90th percentiles, (i) annual 99th percentiles, and (l) annual maxima. The overall mean value is marked with a dot. The annual mean is found to go down under both scenarios, but more so for RCP8.5 (Figures 3a and 3b). However, the variance goes up (see Figure 3c), and again more so for RCP8.5. This makes the wave field more variable even though the mean values appear to go down. This impression is confirmed by the figures (Figures 3f and 3i) for the annual upper percentiles and annual maxima (Figure 3l).

5%. Figure 3 shows the RCP4.5 (left) and RCP8.5 scenarios (right). The projected changes in H_s over the period 2071–2100 relative to the period 1971–2000 is presented (from the top) by the mean, p90, p99, and annual maximum. It is evident that the annual mean wave height is projected to decrease over the majority of the northeast Atlantic (colored areas have statistically significant changes) while increasing wave conditions are expected to the north due to a retreating marginal ice zone (MIZ)—a direct result of global warming [Thomson and Rogers, 2014; Khon *et al.*, 2014]. Higher percentiles see smaller changes under both scenarios. For RCP4.5, almost no significant change is detected for the annual maximum. This suggests that decreasing mean wave conditions does not necessarily lead to decreasing extremes. Simply put, the variance may go up while the mean is reduced, leading to lower annual mean wave height and higher extremes. This is clearly seen in Figures 3c, 3f, 3i, and 3l where the slope of the quantile-quantile plots indicates higher future variance.

To compare integrations forced with winds from climate models with differing biases and levels of model activity (variance), we standardize the climate projections against the historical period,

$$\frac{H_t - \bar{H}_{\text{Hist}}}{\text{std}(H_{t,\text{Hist}})}, \quad (2)$$

where $H_{t,\text{Hist}}$ represents H_t over the historical period only. This transforms annual maxima into annual Z-scores, where each entry represents the number of standard deviations away from the historical mean (here using the sample mean and sample standard deviation as an estimator for the true population equivalent). In the following, we consider extremes with a recurrence rate of once every 10 or 20 years, i.e., annual probability of nonexceedance $1-10^{-1}$ and $1-20^{-1}$, or equivalently the 90 and 95 percentile (hereafter referred to as p90 and p95) of the annual maxima data. As each model is represented by ~ 30 annual entries within each period, estimates of the p90 and p95 will be approximated by the interpolated value of the third and fourth highest entry and the second highest entry (assuming the plotting position $P = (m - 0.5)/N$ [Makkonen, 2006], where m being the rank and N being the total number of entries), respectively. In this way, the 10 and 20 year return value estimates are obtained without resorting to any extreme value models. In Figure 4, we present the discrepancy in p90 and p95 Z-scores between the historical period and the two RCP scenarios, here represented by the median Z-score from the six models at each grid box. In addition, grid boxes where five out of six models agree on sign, i.e., indicating either an increase or a decrease in the future climate, is marked by a black dot (every second grid box). It is shown that the RCP4.5 scenario is projecting an increase in return value estimates within the central parts of the North Atlantic, west of the British Isles. For the 10 year return, the increase is mainly within one standard deviation of the historical climate, while the 20 year return exceeds one standard deviation over a larger area. Similarly, the analysis indicates an increase in the southern coastal areas of Norway, again, with a stronger increase for the longer return period. Areas to the north where the increase exceeds one standard deviation are mainly an effect of the retreating ice cover. Overall, the RCP8.5 shows a slightly less organized result but exhibits a somewhat stronger retreat in ice cover with a corresponding increase in wave height (not visible as historical ice extent masks future open areas).

5. Conclusions

In this study, wave model simulations covering the northeast Atlantic have been conducted using 3-hourly near-surface winds obtained from six CMIP5 models. The model ensemble covers the time slices 1971–2000 and 2071–2100, where the latter is based on two climate scenarios, RCP4.5 and RCP8.5. By comparing the simulated historical wave climate against NORA10, we find that the six CMIP5 models provide quite different forcings. On the basis of mean significant wave height in the historical period, EC-Earth is found to perform best. This is in line with Perez *et al.* [2014] who found EC-Earth to be the one among our six which most faithfully reproduced spatial patterns in sea level pressure variability in the northeast Atlantic. This is also in line with what is found by Zappa *et al.* [2013a], where the CMIP5 models are evaluated in terms of extratropical cyclone activity.

A “well-behaving” historical climate integration does not guarantee its future behavior. For instance, different radiative forcing may introduce different model behavior. Conversely, bias in the historical period should not automatically disqualify a model as it may still be able to reproduce relative changes with time.

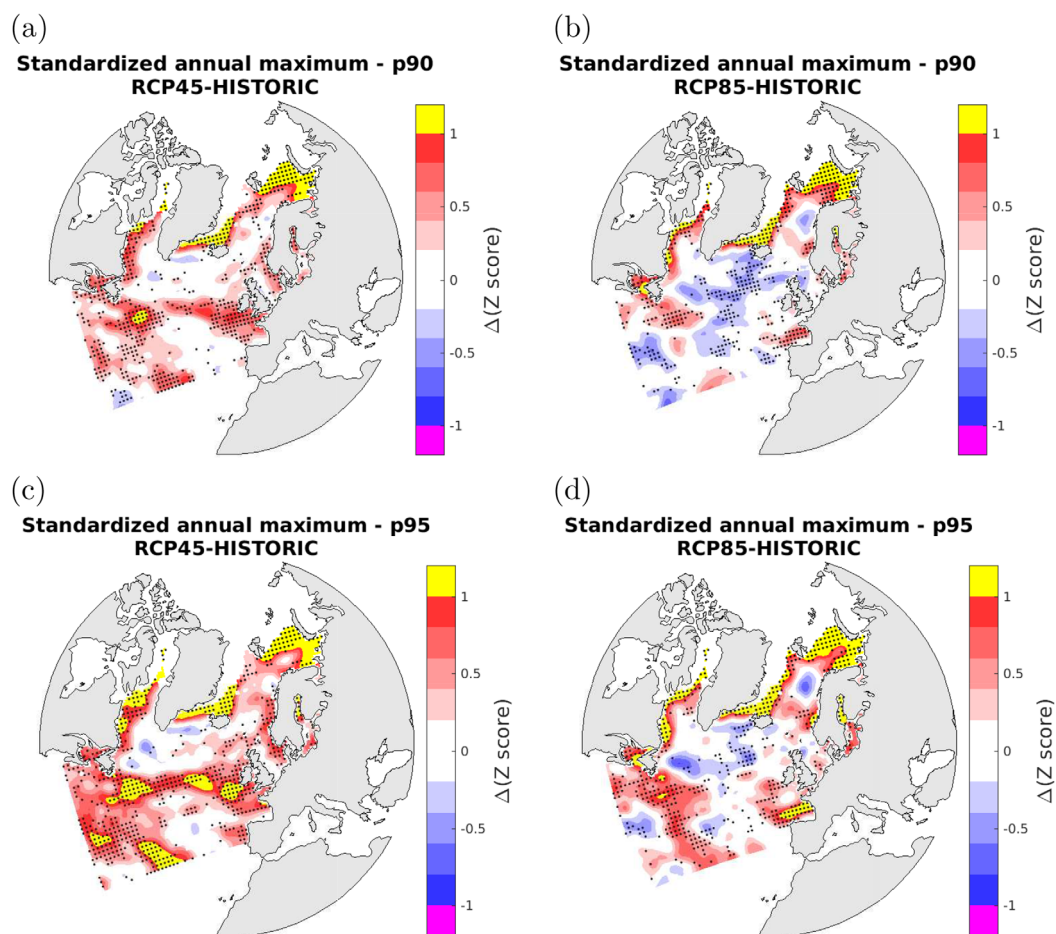


Figure 4. Standardized difference in extreme significant wave height between periods 2071–2100 and the historical period 1971–2000. (a, b) The 10 year return values for scenarios RCP4.5 and 8.5, respectively. As each model integration represents about 30 years, the 10 year return value falls between the third and fourth-highest entries, or the 90th percentile of the entire period. (c, d) The 20 year return values for RCP4.5 and RCP8.5, respectively (which will fall close to the second-highest entry in a 30 year series, or approximately the 95th percentile of the entire 30 year period). Hatching indicates regions where five out of six models agree on the sign of the difference. The results are more patchy than the annual 99th percentiles shown in Figures 3j and 3k, but the pattern is the same, with RCP4.5 revealing slightly higher return values than RCP8.5.

Therefore, in this study, all six models are put together in a model ensemble where each individual model is weighted equally, independent of the model performance relative to NORA10, and standardized relative to the historical climate of each model.

From the future model ensemble, we find a decrease in significant wave height in the northeast Atlantic by the end of the 21st century. This decrease is most prominent under the RCP8.5 scenario, similar to that presented by *Dobrynin et al.* [2012], and probably linked to the enhanced warming of the Arctic [*Overland et al.*, 2014], which reduces the temperature gradient between the Arctic and extratropical regions and further reduce baroclinic instability and cyclogenesis [*Seiler and Zwiers*, 2015]. Although the RCP4.5 will promote the same effects, it will be weaker as the Arctic region is not expected to experience the same warming. Both scenarios indicate the largest changes in significant wave height near the mean, while the tendency is weaker going into the upper tail of the distribution. In particular, RCP4.5 shows little or no significant changes in annual maxima. This feature, based on RCP4.5, is confirmed by *Zappa et al.* [2013b], where it is shown that the projected mean wind intensity related to extratropical cyclones is decreasing, while the average wind intensity related to the strongest extratropical cyclones remains mostly unchanged in the North Atlantic. In contrast, the RCP8.5 shows a significant decrease in annual maxima. This is in line with *Seiler and Zwiers* [2015], who reported an average decrease of 17% in future Atlantic explosive extratropical cyclone frequency. Beyond the annual maximum, i.e., extremes corresponding to return periods of

10 and 20 years, the results are more patchy geographically. Still, for RCP4.5, we find an increase west of the British Isles, where at least five out of six models agree on sign. Locally, these extremes are approximately one standard deviation higher in the future climate. A similar, but weaker increase is found in the southern coastal areas of Norway. Again, changes based on RCP8.5 are more moderate and the signal is less organized, which suggests an unaltered future extreme wave climate.

This study shows that in the central North Atlantic, the mean significant wave height can be expected to decrease by between ~6% (RCP4.5) and ~10% (RCP8.5), relative to the reference period (1971–2000), by the end of the century. The North Sea exhibits a decrease of 2–4% in the western part, otherwise nonsignificant changes. This is in line with *Sterl et al.* [2015] and *Winter et al.* [2013]. The eastern Norwegian Sea also shows a decrease of 2–4% near Haltenbanken, otherwise nonsignificant changes, while the western Norwegian Sea and the Barents Sea see increasing wave heights caused by the retreating marginal ice zone. For the annual maxima, only RCP8.5 shows significant changes compared to the historical period, with a 6–8% decrease in the central North Atlantic.

Acknowledgments

The CMIP5 wind and sea ice data are available at http://cmip-pcmdi.llnl.gov/cmip5/data_portal.html. The wave model simulations (~2 TB) are archived at the Norwegian Meteorological Institute and can be accessed on request. This study was carried out with support from the Research Council of Norway through the ExWaCli project (grant 226239) and later the ExWaMar project (grant 256466). A big thanks to Clause Wyser at SMHI for providing EC-Earth data. We thank the two anonymous reviewers for their constructive comments.

References

- Aarnes, O. J., O. Breivik, and M. Reistad (2012), Wave extremes in the northeast Atlantic, *J. Clim.*, *25*, 1529–1543, doi:10.1175/JCLI-D-11-00132.1.
- Barros, V., et al. (2014), Climate change 2014: Impacts, adaptation, and vulnerability, Part b: Regional aspects, in *Contribution of Working Group II to the Fifth Assessment Report of the Intergovernmental Panel on Climate Change*, edited by V. R. Barros et al., pp. 688, Cambridge Univ. Press, Cambridge, U. K.
- Breivik, Ø., O. J. Aarnes, J.-R. Bidlot, A. Carrasco, and Ø. Sætra (2013), Wave extremes in the northeast Atlantic from ensemble forecasts, *J. Clim.*, *26*(19), 7525–7540, doi:10.1175/JCLI-D-12-00738.1.
- Breivik, Ø., O. J. Aarnes, S. Abdalla, J.-R. Bidlot, and P. A. Janssen (2014), Wind and wave extremes over the world oceans from very large ensembles, *Geophys. Res. Lett.*, *41*, 5122–5131, doi:10.1002/2014GL060997.
- Breivik, Ø., K. Mogensen, J.-R. Bidlot, M. A. Balmaseda, and P. A. Janssen (2015), Surface wave effects in the NEMO ocean model: Forced and coupled experiments, *J. Geophys. Res. Oceans*, *120*, 2973–2992, doi:10.1002/2014JC010565.
- Casas-Prat, M., and J. Sierra (2013), Projected future wave climate in the NW Mediterranean Sea, *J. Geophys. Res. Oceans*, *118*, 3548–3568, doi:10.1002/jgrc.20233.
- Cavaleri, L., B. Fox-Kemper, and M. Hemer (2012), Wind waves in the coupled climate system, *Bull. Am. Meteorol. Soc.*, *93*(11), 1651–1661, doi:10.1175/BAMS-D-11-00170.1.
- Dobrynin, M., J. Murawsky, and S. Yang (2012), Evolution of the global wind wave climate in CMIP5 experiments, *Geophys. Res. Lett.*, *39*, L18606, doi:10.1029/2012GL052843.
- Dufresne, J.-L., et al. (2013), Climate change projections using the IPSL-CM5 earth system model: From CMIP3 to CMIP5, *Clim. Dyn.*, *40*(9–10), 2123–2165, doi:10.1007/s00382-012-1636-1.
- Erikson, L. H., C. Hegermiller, P. Barnard, P. Ruggiero, and M. van Ormondt (2015), Projected wave conditions in the eastern north pacific under the influence of two CMIP5 climate scenarios, *Ocean Modell.*, *96*, 171–185, doi:10.1016/j.ocemod.2015.07.004.
- Fan, Y., and S. M. Griffies (2014), Impacts of parameterized Langmuir turbulence and nonbreaking wave mixing in global climate simulations, *J. Clim.*, *27*(12), 4752–4775, doi:10.1175/JCLI-D-13-00583.1.
- Fan, Y., I. M. Held, S.-J. Lin, and X. L. Wang (2013), Ocean warming effect on surface gravity wave climate change for the end of the twenty-first century, *J. Clim.*, *26*(16), 6046–6066, doi:10.1175/JCLI-D-12-00410.1.
- Fan, Y., S.-J. Lin, S. M. Griffies, and M. A. Hemer (2014), Simulated global swell and wind-sea climate and their responses to anthropogenic climate change at the end of the twenty-first century, *J. Clim.*, *27*(10), 3516–3536, doi:10.1175/JCLI-D-13-00198.1.
- Furevik, B. R., and H. Haakenstad (2012), Near-surface marine wind profiles from rawinsonde and NORA10 hindcast, *J. Geophys. Res. Atmos.*, *117*, D23106, doi:10.1029/2012JD018523.
- Gallagher, S., E. Gleeson, R. Tiron, R. McGrath, and F. Dias (2016), Wave climate projections for Ireland for the end of the 21st century including analysis of EC-Earth winds over the North Atlantic Ocean, *Int. J. Climatol.*, *36*(14), 4592–4607, doi:10.1002/joc.4656.
- Grabemann, I., N. Groll, J. Möller, and R. Weisse (2015), Climate change impact on North Sea wave conditions: A consistent analysis of ten projections, *Ocean Dyn.*, *65*(2), 255–267, doi:10.1007/s10236-014-0800-z.
- Group, T. W. (1988), The WAM model—A third generation ocean wave prediction model, *J. Phys. Oceanogr.*, *18*(12), 1775–1810, doi:10.1175/1520-0485(1988)018<1775:TWMTGO>2.0.CO;2.
- Hasselmann, K., et al. (1973), Measurements of wind-wave growth and swell decay during the joint North Sea Wave Project (JONSWAP), technical report, *Deut. Hydrogr. Z.*, *8*(12), 1–95.
- Hemer, M. A., and C. E. Trenham (2016), Evaluation of a CMIP5 derived dynamical global wind wave climate model ensemble, *Ocean Modell.*, *103*, 190–203, doi:10.1016/j.ocemod.2015.10.009.
- Hemer, M. A., X. L. Wang, R. Weisse, and V. R. Swail (2012), Advancing wind-waves climate science: The COWCLIP project, *Bull. Am. Meteorol. Soc.*, *93*(6), 791–796, doi:10.1175/BAMS-D-11-00184.1.
- Hemer, M. A., Y. Fan, N. Mori, A. Semedo, and X. L. Wang (2013), Projected changes in wave climate from a multi-model ensemble, *Nat. Clim. Change*, *3*(5), 471–476, doi:10.1038/nclimate1791.
- Hurrell, J. W. (1995), Decadal trends in the North Atlantic oscillation, *Science*, *269*, 676–679, doi:10.1126/science.269.5224.676.
- Kalnay, E., et al. (1996), The NCEP/NCAR reanalysis 40-year project, *Bull. Am. Meteorol. Soc.*, *77*(3), 437–471, doi:10.1175/1520-0477(1996)077<0437:TNYRP>2.0.CO;2.
- Khon, V., I. Mokhov, F. Pogarskiy, A. Babanin, K. Dethloff, A. Rinke, and H. Matthes (2014), Wave heights in the 21st century Arctic Ocean simulated with a regional climate model, *Geophys. Res. Lett.*, *41*, 2956–2961, doi:10.1002/2014GL059847.
- Komen, G. J., M. Cavaleri, M. Donelan, K. Hasselmann, S. Hasselmann, and P. A. E. M. Janssen (1994), *Dynamics and Modelling of Ocean Waves*, pp. 554, Cambridge Univ. Press, Cambridge, U. K.

- Li, Q., A. Webb, B. Fox-Kemper, A. Craig, G. Danabasoglu, W. G. Large, and M. Vertenstein (2016), Langmuir mixing effects on global climate: WAVEWATCH III in CESM, *Ocean Modell.*, *103*, 145–160.
- Makkonen, L. (2006), Plotting positions in extreme value analysis, *J. Appl. Meteor. Climatol.*, *45*(2), 334–340, doi:10.1175/JAM2349.1.
- Martínez-Asensio, A., M. Marcos, M. N. Tsimplis, G. Jordà, X. Feng, and D. Gomis (2016), On the ability of statistical wind-wave models to capture the variability and long-term trends of the North Atlantic winter wave climate, *Ocean Modell.*, *103*, 177–189, doi:10.1016/j.ocemod.2016.02.006.
- Mori, N., T. Shimura, T. Yasuda, and H. Mase (2013), Multi-model climate projections of ocean surface variables under different climate scenarios—Future change of waves, sea level and wind, *Ocean Eng.*, *71*, 122–129, doi:10.1016/j.oceaneng.2013.02.016.
- Overland, J. E., M. Wang, J. E. Walsh, and J. C. Stroeve (2014), Future arctic climate changes: Adaptation and mitigation time scales, *Earth's Future*, *2*(2), 68–74, doi:10.1002/2013EF000162.
- Pachauri, R. K., et al. (2014), *Climate Change 2014: Synthesis Report. Contribution of Working Groups I, II and III to the Fifth Assessment Report of the Intergovernmental Panel on Climate Change*, edited by Core Writing Team, R. K. Pachauri, and L. A. Meyer, 151 pp., Geneva, Switzerland.
- Perez, J., M. Menendez, F. J. Mendez, and I. J. Losada (2014), Evaluating the performance of CMIP3 and CMIP5 global climate models over the North-East Atlantic region, *Clim. Dyn.*, *43*(9–10), 2663–2680, doi:10.1007/s00382-014-2078-8.
- Perez, J., M. Menendez, P. Camus, F. J. Mendez, and I. J. Losada (2015), Statistical multi-model climate projections of surface ocean waves in Europe, *Ocean Modell.*, *96*, 161–170, doi:10.1016/j.ocemod.2015.06.001.
- Reistad, M., O. Breivik, H. Haakenstad, O. J. Aarnes, and B. R. Furevik (2011), A high-resolution hindcast of wind and waves for the North Sea, the Norwegian Sea and the Barents Sea, *J. Geophys. Res.*, *116*, C05019, doi:10.1029/2010JC006402.
- Seiler, C., and F. Zwiers (2015), How will climate change affect explosive cyclones in the extratropics of the Northern Hemisphere?, *Clim. Dyn.*, *46*, 3633–3644, doi:10.1007/s00382-015-2791-y.
- Semedo, A., R. Weisse, A. Behrens, A. Sterl, L. Bengtsson, and H. Günther (2012), Projection of global wave climate change toward the end of the twenty-first century, *J. Clim.*, *26*(21), 8269–8288, doi:10.1175/JCLI-D-12-00658.1.
- Shimura, T., N. Mori, and H. Mase (2013), Ocean waves and teleconnection patterns in the Northern Hemisphere, *J. Clim.*, *26*(21), 8654–8670, doi:10.1175/JCLI-D-12-00397.1.
- Shimura, T., N. Mori, and H. Mase (2015a), Future projections of extreme ocean wave climates and the relation to tropical cyclones: Ensemble experiments of MRI-AGCM3.2H, *J. Clim.*, *28*(24), 9838–9856, doi:10.1175/JCLI-D-14-00711.1.
- Shimura, T., N. Mori, and H. Mase (2015b), Future projection of ocean wave climate: Analysis of SST impacts on wave climate changes in the western North Pacific, *J. Clim.*, *28*(8), 3171–3190, doi:10.1175/JCLI-D-14-00187.1.
- Shimura, T., N. Mori, and M. A. Hemer (2016), Variability and future decreases in winter wave heights in the western North Pacific, *Geophys. Res. Lett.*, *43*, 2716–2722, doi:10.1002/2016GL067924.
- Sterl, A., A. M. Bakker, H. W. van den Brink, R. Haarsma, A. Stepek, I. L. Wijnant, and R. C. de Winter (2015), Large-scale winds in the southern North Sea region: The wind part of the KNMI 14 climate change scenarios, *Environ. Res. Lett.*, *10*(3), 035004.
- Stocker, T. F., D. Qin, G.-K. Plattner, M. Tignor, S. K. Allen, J. Boschung, A. Nauels, Y. Xia, V. Bex, and P. M. Midgley (2014), Climate change 2013: The physical science basis, in *Contribution of Working Group I to the Fifth Assessment Report of the Intergovernmental Panel on Climate Change*, edited by T. F. Stocker et al., 1535 pp., Cambridge Univ. Press, Cambridge, U. K.
- Stopa, J. E., K. F. Cheung, H. L. Tolman, and A. Chawla (2013), Patterns and cycles in the climate forecast system reanalysis wind and wave data, *Ocean Modell.*, *70*, 207–220, doi:10.1016/j.ocemod.2012.10.005.
- Taylor, K. E., R. J. Stouffer, and G. A. Meehl (2012), An overview of CMIP5 and the experiment design, *Bull. Am. Meteorol. Soc.*, *93*(4), 485.
- Thomson, J., and W. E. Rogers (2014), Swell and sea in the emerging arctic ocean, *Geophys. Res. Lett.*, *41*, 3136–3140, doi:10.1002/2014GL059983.
- Uppala, S. M., et al. (2005), The ERA-40 re-analysis, *Q. J. R. Meteorol. Soc.*, *131*(612), 2961–3012, doi:10.1256/qj.04.176.
- Wang, X. L., Y. Feng, and V. R. Swail (2014), Changes in global ocean wave heights as projected using multimodel CMIP5 simulations, *Geophys. Res. Lett.*, *41*, 1026–1034, doi:10.1002/2013GL058650.
- Wang, X. L., Y. Feng, and V. R. Swail (2015), Climate change signal and uncertainty in CMIP5-based projections of global ocean surface wave heights, *J. Geophys. Res. Oceans*, *120*, 3859–3871, doi:10.1002/2015JC010699.
- Winter, R. D., A. Sterl, and B. Ruessink (2013), Wind extremes in the North Sea basin under climate change: An ensemble study of 12 CMIP5 GCMS, *J. Geophys. Res. Atmos.*, *118*, 1601–1612, doi:10.1002/jgrd.50147.
- Zappa, G., L. C. Shaffrey, and K. I. Hodges (2013a), The ability of CMIP5 models to simulate North Atlantic extratropical cyclones, *J. Clim.*, *26*(15), 5379–5396, doi:10.1175/JCLI-D-12-00501.1.
- Zappa, G., L. C. Shaffrey, K. I. Hodges, P. G. Sansom, and D. B. Stephenson (2013b), A multimodel assessment of future projections of North Atlantic and European extratropical cyclones in the CMIP5 climate models, *J. Clim.*, *26*(16), 5846–5862, doi:10.1175/JCLI-D-12-00573.1.